DOI: 10.26599/FSHW.2026.9250959

Contents lists available at SciOpen

Food Science and Human Wellness

journal homepage: https://www.sciopen.com/journal/2097-0765

China Food Publishing Co.

Glyphosate induces lipid metabolism imbalance in liver of zebrafish (*Danio rerio*) under different dietary conditions: Unexpected discovery from the perspective of the gut-liver axis

Yuntong Gu [a, 1], Yaowen Cui [a, 1], Xiayun Wang [a], Lei Wang [a], Yixuan Zou [a], Qian Zeng [a], Li Liu [c], Xiaojun Chen [a, b], Zhiyuan Meng [a, b] *

[a] *College of Plant Protection / Jiangsu Province Engineering Research Center of Green Pesticides, Yangzhou University, Yangzhou, Jiangsu 225009, China*

[b] *Intelligence Agriculture Interdisciplinary Center of Yangzhou University, Yangzhou, Jiangsu 225009, China*

[c] *School of Tourism and Cuisine, Yangzhou University, Jiangsu, Yangzhou 225127, China*

ABSTRACT: Glyphosate (GLY) is a widely used herbicide worldwide, whose environmental risks cannot be ignored. In this study, the adverse effects of GLY on the liver function of zebrafish were systematically investigated from the perspective of the gut-liver axis under normal diet (6% crude fat) and high-fat diet conditions (HFD, 24% crude fat). Combined histopathological and physiological biochemical analysis revealed that GLY exposure caused structural damage and an inflammatory response in the liver of zebrafish, accompanied by significant lipid accumulation. Analysis of the expression of metabolic phenotypes and lipid homeostasis-related genes in the liver of zebrafish revealed that GLY caused a disorder of the liver metabolic profiles. This disorder led to significant changes in the contents of metabolites associated with lipid and amino acid metabolism under normal diet and high-fat diet conditions. GLY exposure also promoted the expression of genes associated with fatty acid synthesis and inhibited the expression of genes associated with fatty acid oxidation in the liver of zebrafish. Analysis of intestinal function revealed that GLY exposure led to intestinal dysfunction and ecological imbalances of gut microbiota in zebrafish. Correlation analysis revealed close relationships between changes in the composition of gut microbiota and changes in liver function under GLY exposure. The combined exposure of GLY and HFD caused more severe toxicity effects, including liver damage, intestinal barrier damage, and dysbiosis of the gut microbiota in zebrafish. These results reveal the effects of GLY exposure on liver function, intestinal barrier function, and gut microbiota composition of zebrafish under different dietary conditions and provide new insights into the mechanism of regulating GLY-induced hepatotoxicity via the gut-liver axis. The findings of this study deepen our understanding of the environmental risks of GLY and underscore the influence of different dietary conditions on the toxicity effects of pesticides.

Keywords: glyphosate, liver function, lipid metabolism, intestinal barrier, gut microbiota

1. Introduction

Glyphosate (GLY) is a popular herbicide product widely used in agriculture, forestry, and horticulture [1]. Its global annual usage in 2020 was 0.75 million tons, and is expected to reach 0.90 million tons by 2025 [2].

[1] Yuntong Gu and Yaowen Cui contributed equally to this work.
***Corresponding author**
Zhiyuan Meng, E-mail: zymeng@yzu.edu.cn

Received 18 March 2025
Received in revised from 20 April 2025
Accepted 13 October 2025

The extensive use of GLY has led to its entry into the environmental medium through water circulation, causing a certain degree of pollution to soil and water bodies. For instance, the concentration of GLY in the soils of Hunan, Zhejiang, and Guangxi provinces ranges between 130 and 910 μg/kg [3]. In agricultural watersheds of 10 provinces in China, the detection rate of GLY in 694 groundwater samples was 1.01%, with a maximum concentration of 2.09 μg/L. And the detection rate of GLY in 196 surface water samples was 14.3%, with a maximum concentration of 32.49 μg/L [4]. Notably, GLY is also enriched in food [5]. Studies postulate that GLY has been detected in 34% of food samples, such as fruits, vegetables, and grains. The residual concentration of GLY in soybeans and corn is 3.26 and 0.07 mg/kg, respectively [6]. Due to its widespread presence in environmental media, the potential health risks of GLY are receiving increasing attention. Studies postulate that the occurrence of many diseases is closely associated with GLY pollution [7]. Epidemiological studies postulate that the occurrence of clinical diseases, such as celiac disease, obesity, and cancer, is related to GLY exposure [8]. Moreover, GLY can cause gut microbiota dysbiosis, leading to metabolic abnormalities or neurological disorders [9]. GLY also enhances the proliferation of estrogen-dependent MCF-7 breast cancer cells [10]. GLY also induces the occurrence of uterine hyperplasia or leiomyoma in mice [11]. Non-targeted lipidomics studies report that GLY causes liver toxicity symptoms, leading to abnormal increases in total bile acids, triglycerides, and other indicators, indicating that lipids in the organism are continuously accumulating [12]. Noteworthy, GLY has been detected in the brains of orally administered GLY mice, indicating that GLY can cross the blood-brain barrier and exert neurotoxic effects [13]. These reports confirm that GLY is transmitted via the food chain and significantly impacts physiological metabolism, growth, and development. As such, the health risks caused by dietary intake of GLY cannot be ignored.

People's living standards have gradually improved in the past 30 years, and their dietary habits have also changed, shifting from a traditional low-fat and carbohydrate-rich diet to a low-fat and high-fat diet. Today, high-fat diets are common among young people [14]. A high-fat diet has a negative impact on human health. It reduces the abundance of gut microbiota, causing an increase in serum total cholesterol, low-density lipoprotein cholesterol, and non-high-density lipoprotein cholesterol levels, leading to metabolic abnormalities [15]. A high-fat diet can also lead to visceral fat accumulation, insulin resistance, oxidative stress, and cognitive impairment. These factors lead to chronic diseases, with a mortality rate of up to 70% [16]. Studies postulate that triclosan and triclocarban cause liver lipid damage in mice. High-fat-fed mice exhibit significant changes in liver indicators compared to the low-fat-fed mice, highlighting the exacerbation of the toxic effects of high-fat diet on triclosan and triclocarban [17]. Furthermore, treatment with the insecticide chlorpyrifos induced metabolic abnormalities in mice, including elevated glucose levels. The high-fat diet group exhibited greater increases in ATP consumption, liver ALT and AST levels compared to the low-fat diet group, indicating that high-fat intake exacerbates chlorpyrifos toxicity [18]. The combined effect of GLY and a high-fat diet is crucial because GLY is a common residual pesticide in food. Importantly, glyphosate and high-fat diet can significantly interfere with lipid metabolism in the body. Glyphosate can affect lipid

oxidation and synthesis, leading to abnormal accumulation of liver lipids in organisms. A high-fat diet directly provides excessive lipids, leading to metabolic overload in the body. However, studies on the interaction between GLY and a high-fat diet remain limited. Analyzing the relationship between the two has significant research significance.

The gut microbiota is important to energy absorption because it converts food into the nutrients the body needs [19]. There is a symbiotic relationship between the body and gut microbiota. The body will exhibit different pathological states based on the diversity and abundance of gut microbiota [20]. Studies postulate that rats exposed to environments containing different concentrations of chlorpyrifos or regularly fed on high-fat diets experience dysbiosis and a decrease in the abundance of the gut microbiota, leading to metabolic disorders. Notably, these changes are more pronounced in the high-fat-fed mice [21]. Gut microbiota disrupts lipid metabolism in mouse intestines by inhibiting the expression of long-chain non-coding RNA in small intestinal epithelial cells. This phenomenon explains why mice lacking gut microbiota are less likely to gain weight under a high-fat diet [22]. Gut microbiota thus plays an extremely important role in metabolic research. Exploring the combined effect of GLY exposure and a high-fat diet from the perspective of gut microbiota is thus necessary.

In this study, zebrafish were used as a model organism to explore the effects of GLY exposure at different concentrations and dietary conditions on lipid metabolism, focusing on deciphering the combined harm of GLY and a high-fat diet to the organism. This study reveals the interaction between GLY exposure and a high-fat diet, providing more comprehensive data for GLY toxicity research.

2. Materials and methods

2.1 Chemicals and reagents

Glyphosate (GLY, purity $\geqslant$ 99%) was purchased from Sigma-Aldrich (Sigma, USA). The normal diet (ND, 6% crude fat) and high fat diet (HFD, 24% crude fat) of zebrafish were supported by Shandong Yixiyue Biotechnology Co., Ltd (Shandong, China). And other chemical reagents were obtained from Aladdin Biotech (Shanghai, China). RNA extraction and qPCR analysis kits were sourced from Tiangen Biotech (Beijing, China). The water used in all experiments was purified using a Milli-Q water purification system (Millipore, USA).

2.2 Zebrafish maintenance and experimental design

Artificially cultivated male zebrafish (four-month-old, wild-type strain) were purchased from the Huaduhui Aquarium Supermarket (Yangzhou, China). The zebrafish were domesticated at a constant temperature water environment of 28 $\pm$ 0.5℃ with a light/dark cycle of 14/10 hours for 2 weeks. During the 1 week of adaptive feeding, zebrafish were fed twice daily during the domestication process. Feeding was stopped 24 hours before the start of the experiment. They were randomly divided into six treatment groups (n = 100 per group) after domestication for experimental purposes. Zebrafish in three treatment groups were fed a normal diet (ND, 6% crude fat) twice daily and subjected to three GLY exposure levels (0, 50, and 500

μg/L). Here, a large number of previous studies have shown that the concentration range of GLY detected in groundwater and surface water at home and abroad is 1.8 to 427 μg/L [23, 24]. Therefore, we set 500 μg/L as the highest exposure concentration for this study, and 50 μg/L as the lowest exposure concentration for this study. These treatment groups were designated as the Control (Ctrl), L-GLY, and H-GLY treatment groups, respectively. The other three treatment groups were fed a high-fat diet (HFD, 24% crude fat) twice daily and subjected to three GLY exposure levels (0, 50, and 500 μg/L). These treatment groups were designated as High-fat diet (HFD), L-GLY+HFD, and H-GLY+HFD treatment groups, respectively. The water was changed every 2 days to ensure a constant target drug concentration. The exposure experiment lasted for 28 days, after which the zebrafish were anesthetized using MS-222 on ice, followed by determination of their body weight and length. The zebrafish were dissected on ice to collect their intestinal and liver tissues and the cercal contents, which were subsequently stored at -80°C. Sections of the liver and intestinal tissues were fixed in 4% formalin solution for histopathology analysis. The composition and nutritional components of the experimental diet are shown in Table S1.

2.3 Biochemical indicators and histopathology analysis

Livers from five zebrafish in each group were pooled to form one replicate (n = 4, 5 fsh/replicate). Each pooled sample was homogenized in nine volumes of cold saline solution based on its tissue weight, using a homogenizer for 2 minutes. The resulting homogenate was then centrifuged at 3,500 rpm for 10 min to collect the supernatant. Then, the contents of total cholesterol (TC), triglyceride (TG), and total bile acid (TBA) in the liver of zebrafish were determined using the respective kits (product IDs: A111-2-1, A110-2-1 and E003-2-1) following the manufacturer's instructions. The kits were purchased from the Nanjing Jiancheng Institute of Biotechnology (Nanjing, China). Histopathological analysis was performed by fixing zebrafish liver and intestinal tissues in 4% formalin solution, followed by dehydration and paraffin embedding. The liver and intestinal tissues were then cut into thin slices (5 μm), which were dewaxed and stained with hematoxylin-eosin (H&E), and subsequently viewed and photographed using the Olympus BX51 imaging system (Olympus Corp.).

2.4 Metabolomics analysis of the liver tissues

Zebrafish liver samples (50 mg) were accurately weighed and extracted twice using 600 μL methanol–water solutions (V: V= 2:1). The supernatants were dried under nitrogen and subsequently redissolved in 550 μL of phosphate buffer (pH 7.4) containing D_2O and TSP-D_4 (1 mM). The extracted metabolomics samples were then analyzed using a Bruker AV III600 NMR spectrometer (Bruker, Billerica, USA). Multivariate statistical analysis was subsequently conducted using SIMCA-P software Version 14.0 and MetaboAnalyst 5.0 [25]. The detailed metabolomics analysis method is outlined in Supporting Information S1.

2.5 Analysis of gut microbiota

The DNA of bacteria in the intestinal contents was extracted using the DNA Stool Mini Kit (Qiagen) according to the manufacturer's instructions. Universal primers 338F (5'-ACTCCTACGGGAGGCGCAGCA-3') and 806R (5'-GGACTACHVGGG TWTCTAAT-3') were used to amplify 16S rDNA to target the V3-V4 genetic region. The PCR products were subsequently sequenced by Shanghai Personal Biotechnology Co., Ltd. (Shanghai, China). The detailed paired-end sequencing method of gut microbiota is outlined in Supporting Information S2.

2.6 Gene expression analysis

The mRNA expression levels of inflammation-related genes (*Ilβ*, *Tnfα*, *Cxcl18β*) in the liver and intestinal tissues, lipid metabolism-related genes (*Fasn*, *Acaca*, *Fabp10a*, *Hmgcra*, *Lpl*, *Fat*, *Cpt1aa*, *Pgcla*, *Pparg*, *Pparab*, *Pparaa*) in the liver tissue, and barrier function-related genes (*Mucin2*, *Zo1*, *Claudin10*) in the intestinal tissue of zebrafish were analyzed using the Bio-Rad CFX 96 PCR system (Bio-Rad). The RNA extraction and reverse transcription steps followed the manufacturer's instructions of the respective kits. The *β-actin* gene was used as the internal control. The gene expression levels were analyzed using the $2^{-\Delta\Delta Ct}$ relative quantification method. The primers of the target genes were purchased from Sangon Biological Engineering Co., Ltd. (Shanghai, China). The primers used and their sequences are listed in Table S2.

2.7 Statistical analysis

Data were analyzed using SPSS 19.0 (IBM, USA) and presented as means ± standard deviation (SD). The statistical differences ($P < 0.05$) between different treatment groups were calculated using one-way ANOVA. Graphs were generated using GraphPad Prism 8.0 (GraphPad Software).

3. Results

3.1 GLY affected the growth of zebrafish under different dietary conditions

The body weight and length of zebrafish significantly increased in the L-GLY, H-GLY, HFD, L-GLY+HFD, and H-GLY+HFD treatment groups compared to the Ctrl group ($F = 8.046$, $P < 0.001$ for Body weight, $F = 2.948$, $P = 0.020$ for Body length) (Fig. 1A and B). Exposure to L-GLY and H-GLY resulted in a significant increase in body weight of zebrafish under high-fat diet conditions ($F = 8.046$, $P < 0.001$) (Fig. 1A). The BMI of zebrafish also exhibited significant changes. L-GLY and H-GLY cause a significant increase in BMI under normal and high-fat diet conditions ($F = 3.898$, $P = 0.043$) (Fig. 1C). In addition, there was a significant increase in the liver weight of zebrafish in the L-GLY+HFD and H-GLY+HFD treatment groups compared to the Ctrl group. The liver weight of zebrafish also significantly increased in the H-GLY+HFD treatment groups compared to the HFD treatment group ($F = 1.256$, $P = 0.045$) (Fig. 1D). In contrast, GLY exposure did not change the liver index of zebrafish under normal and high-fat diet conditions ($F = 4.817$, $P = 0.012$) (Fig. 1E).

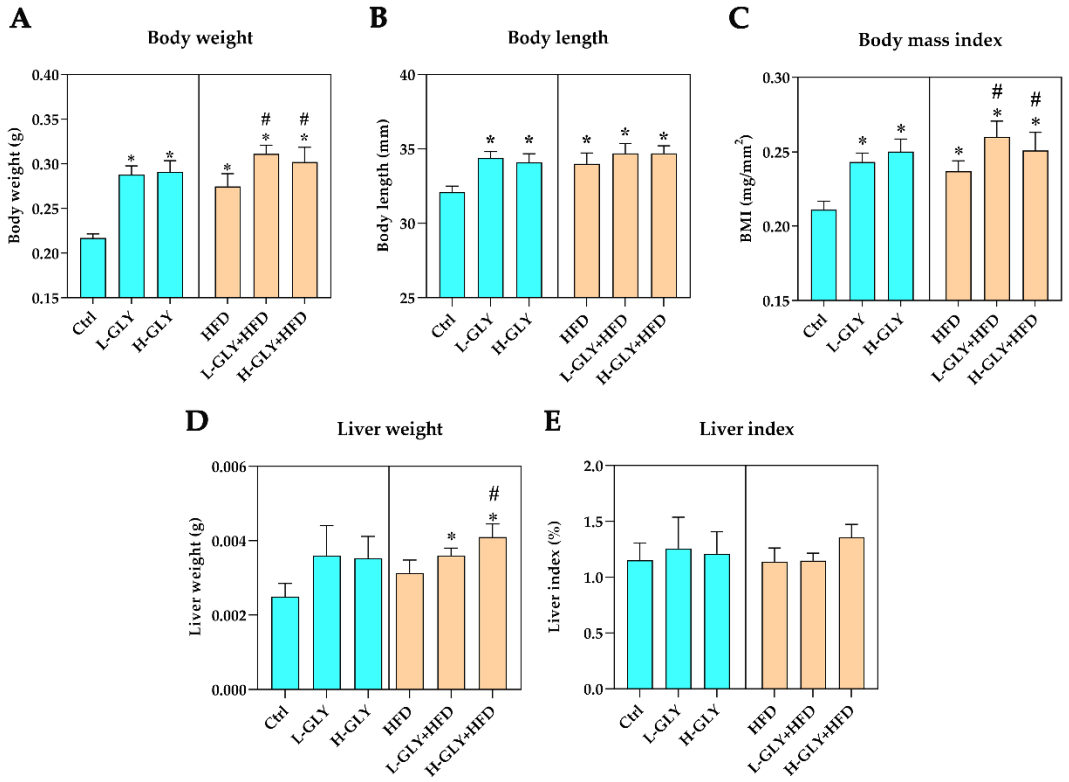

Fig. 1. Exposure to GLY changed physiological parameters of zebrafish. (A) Body weight, (B) Body length, (C) Body mass index, (D) Liver weight, (E) Liver index. Data are expressed as mean ± SD. *P < 0.05 compared with the Ctrl treatment group. $^{\#}P$ < 0.05 compared with the HFD treatment group.

3.2 GLY induced liver damage under different dietary conditions

Histopathological analysis revealed structural disorder in the liver tissue of zebrafish in the L-GLY, H-GLY, HFD, L-GLY+HFD and H-GLY+HFD treatment groups. The liver cells of zebrafish in the L-GLY and H-GLY treatment groups had accumulation of lipid droplets and formation of small amounts of vacuoles. In addition, there were numerous vacuolar degeneration and inflammatory cell infiltration in the liver cells of zebrafish in the L-GLY+HFD and H-GLY+HFD treatment groups (Fig. 2A). L-GLY and H-GLY significantly increased the TC content in the liver of zebrafish under normal and high-fat diet conditions (F = 29.510, P < 0.001) (Fig. 2B). There was a significant increase in the TG content in the liver of zebrafish in the H-GLY, HFD, L-GLY+HFD, and H-GLY+HFD treatment groups compared to the Ctrl group (F = 3.728, P = 0.009) (Fig. 2C). Moreover, there was a significant increase in the TBA content in the liver of zebrafish in the HFD treatment group compared to the Ctrl group. L-GLY and H-GLY significantly reduced the content of TBA in zebrafish fed on a high-fat diet (F=13.320, P < 0.001) (Fig. 2D). In addition, there was significant upregulation of the mRNA expression levels of *Tnfα* and *Il1β* after zebrafish exposure to H-GLY, HFD, L-GLY+HFD, and H-GLY+HFD compared to the Ctrl group (F=6.677, P < 0.001 for *Tnfα*, F=16.720, P < 0.001 for *Il1β*) (Fig. 2E and F). Similarly, there was significant upregulation of the mRNA expression levels of *Tnfα* and *Il1β* in zebrafish in the L-GLY+HFD and H-GLY+HFD treatment groups compared to those in the HFD treatment group (F=6.677, P < 0.001 for *Tnfα*, F = 16.720, P < 0.001 for *Il1β*) (Fig. 2E and F). There was significant upregulation of the mRNA expression levels of *Cxcl18β* in zebrafish in the L-GLY+HFD and H-GLY+HFD treatment groups compared to those in the Ctrl and HFD treatment groups (F=8.486, P < 0.001)

(Fig. 2G). These results demonstrate that exposure to GLY and HFD causes liver injury in zebrafish. Notably, GLY significantly exacerbated liver injury of zebrafish caused by HFD.

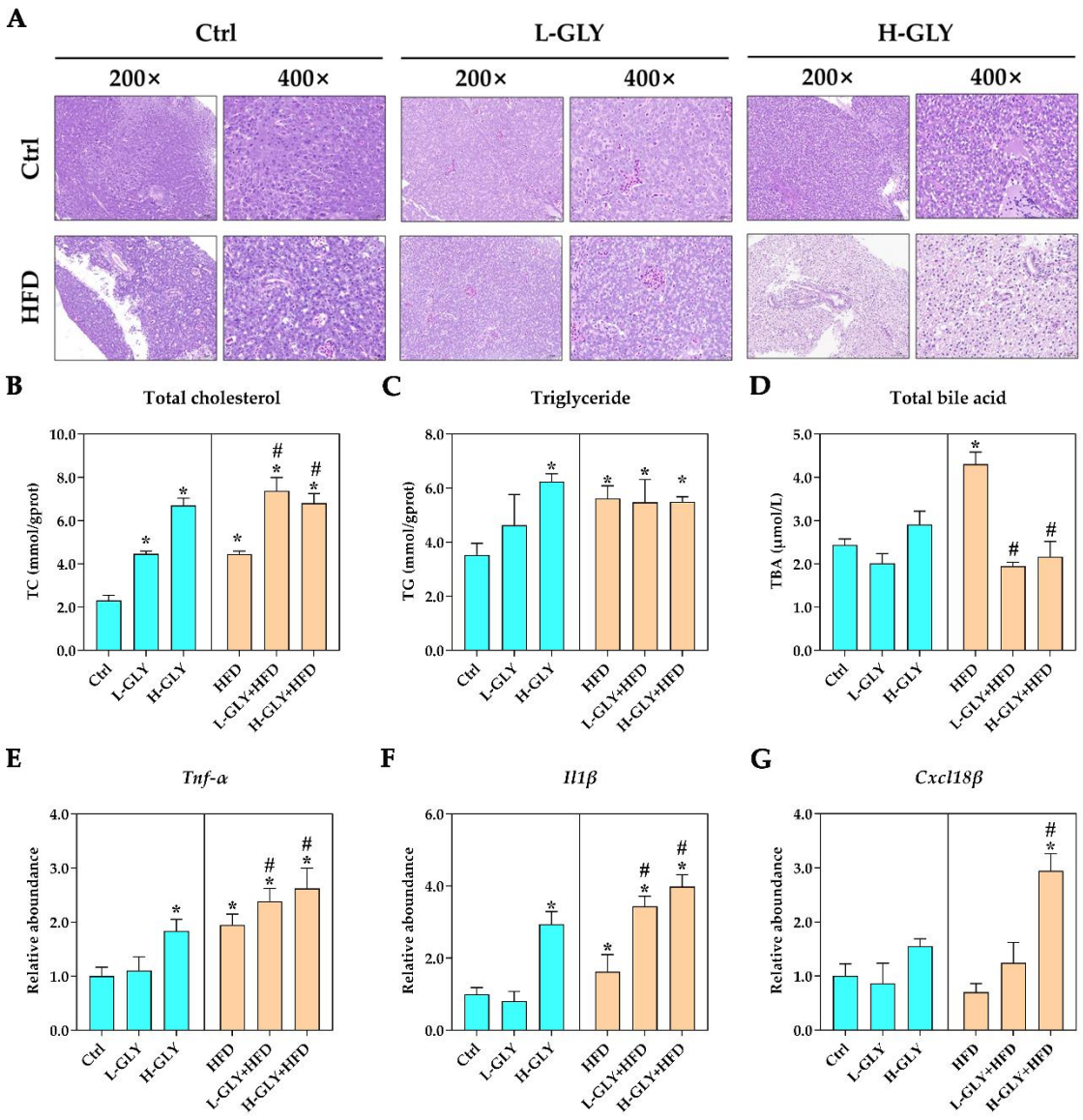

Fig. 2. Exposure to GLY induced liver injury of zebrafish. (A) Representative images of H&E staining of liver tissues, (B) Liver total cholesterol contents, (C) Liver triglyceride contents, (D) Liver total bile acid contents, (E-F) The m RNA expression levels of *Tnfα*, *Il1β* and *Cxcl18β*. Data are expressed as mean ± SD. **P* < 0.05 compared with the Ctrl treatment group. $^{\#}P$ < 0.05 compared with the HFD treatment group.

3.3 GLY disordered the metabolic profiles of the liver under different dietary conditions

The metabolic profiles of liver tissue were analyzed using NMR based on metabolomics technology to further elucidate the effects of GLY on zebrafish liver tissue under different dietary conditions. The representative 600 MHz ^{1}H NMR spectra from liver tissue extracts of zebrafish are depicted in Fig. S1. A total of 42 metabolites were identified based on chemical shifts and peak intensities (Table S3). Notably, there were clear separation trends in the score plots of PCA analysis between the Ctrl group and L-GLY, H-GLY, HFD, L-GLY+HFD, and H-GLY+HFD treatment groups (Fig. 3A). The score plots of OPLS-DA also exhibited clear separation trends between the Ctrl group and the other treatment groups. The OPLS-DA analysis model had good predictability and statistical significance (R_2X = 0.594, R_2Y = 0.992, Q2 = 0.953, and P = 0.009 for

L-GLY treatment groups; R2X = 0.716, R2Y = 0.960, Q2 = 0.862, and P = 0.022 for H-GLY treatment group; R2X = 0.718, R2Y = 0.998, Q2 = 0.973, and P = 0.018 for HFD treatment group; R2X = 0.743, R2Y = 0.993, Q2 = 0.966, and P = 0.005 for L-GLY+HFD treatment group; and R2X = 0.661, R2Y = 0.984, Q2 = 0.858, and P = 0.024 for H-GLY+HFD treatment group) (Fig. 3B-F). Metabolites with significant changes between L-GLY, H-GLY, HFD, L-GLY+HFD, and H-GLY+HFD treatment groups and the Ctrl group were also identified using the Student's t test and volcano plots (Fig. 3B-F).

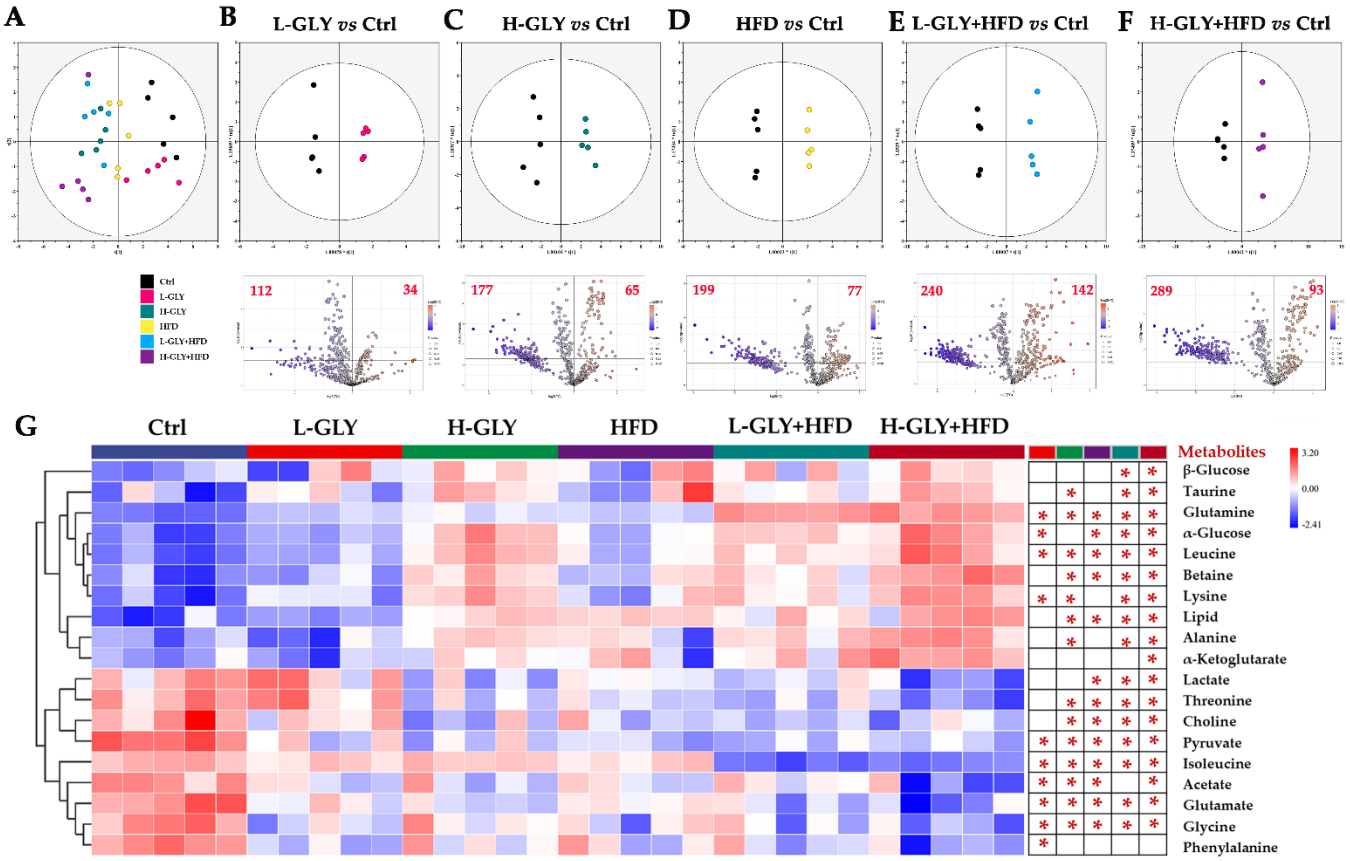

Fig. 3. Exposure to GLY disordered metabolic profiles in liver of zebrafish. (A) The score plot of PCA models, (B-F) OPLS-DA scored plots and corresponding volcano plot were obtained from pairwise comparisons between L-GLY and Ctrl, H-GLY and Ctrl, HFD and Ctrl, L-GLY+HFD and Ctrl, H-GLY+HFD and Ctrl, (G) Heat map for all significantly changed metabolites in liver of zebrafish. Data are expressed as mean ± SD.

In general, 19 metabolites significantly changed in the liver of zebrafish in L-GLY, H-GLY, HFD, L-GLY+HFD, and H-GLY+HFD treatment groups compared to the Ctrl group (Fig. 3G and Table 1). Exposure to L-GLY, H-GLY, HFD, L-GLY+HFD, and H-GLY+HFD resulted in significant changes in 10, 14, 13, 16, and 18 metabolites in the liver of zebrafish, respectively. There was a significant decrease in the relative contents of glutamate, pyruvate, glycine, and isoleucine and a significant increase in the relative contents of glutamine, leucine, lysine, and α-glucose in L-GLY, H-GLY, HFD, L-GLY+HFD, and H-GLY+HFD treatment groups compared to the Ctrl group (Table 1). In addition, exposure to L-GLY and H-GLY significantly increased the relative contents of lipid, taurine, alanine, betaine, and β-glucose. However, it significantly decreased the relative contents of threonine, choline, and lactate in the context of a high-fat diet (Table 1).

Table 1 Identification of significant changed metabolites based on VIP scores and P values of one way ANOVA

Metabolites	L-GLY *vs* Ctrl		H-GLY *vs* Ctrl		HFD *vs* Ctrl		L-GLY+HFD *vs* Ctrl		H-GLY+HFD *vs* Ctrl	
	Fold changes	P values	Fold changes	P values	Fold changes	P values	Fold changes	P values	Fold changes	P values
Lipid	1.07	NS	1.29	*	1.31	*	1.26	*	1.37	*
Threonine	0.99	NS	0.83	*	0.85	*	0.83	*	0.75	*
Acetate	0.81	*	0.81	*	0.83	*	0.86	NS	0.68	*
Glutamate	0.89	*	0.86	*	0.90	*	0.85	*	0.80	*
Glutamine	1.20	*	1.28	*	1.21	*	1.63	*	1.63	*
Pyruvate	0.75	*	0.71	*	0.68	*	0.69	*	0.69	*
α-Ketoglutarate	0.95	NS	1.19	NS	1.15	NS	1.26	NS	1.42	*
Choline	0.92	NS	0.84	*	0.87	*	0.84	*	0.84	*
Taurine	1.21	NS	1.36	*	1.27	NS	1.26	*	1.40	*
Glycine	0.85	*	0.92	*	0.88	*	0.86	*	0.82	*
Isoleucine	0.91	*	0.96	*	0.91	*	0.55	*	0.59	*
Leucine	1.13	*	1.47	*	1.23	*	1.38	*	1.53	*
Lysine	1.16	*	1.34	*	1.17	NS	1.27	*	1.39	*
Alanine	0.98	NS	1.16	*	1.08	NS	1.16	*	1.24	*
Betaine	1.06	NS	1.22	*	1.12	*	1.18	*	1.31	*
Lactate	1.01	NS	0.87	NS	0.92	*	0.89	*	0.82	*
β-Glucose	1.13	NS	1.29	NS	1.23	NS	1.26	*	1.32	*
α-Glucose	1.13	*	1.47	NS	1.22	*	1.42	*	1.52	*
Phenylalanine	0.83	*	0.89	NS	0.88	NS	0.85	NS	0.79	NS

Note: The fold changes of each treatment group against the control group was summarized in Table. *$P < 0.05$ compared with the control group. Red color means significant increased, blue color means significant decrease, and NS means insignificant.

Subsequent enrichment analysis of metabolic pathways was conducted based on significant changes in liver metabolites of zebrafish after exposure to L-GLY, H-GLY, HFD, L-GLY+HFD, and H-GLY+HFD. Fig. 4A-E outlines the top 25 metabolic pathways that changed. The results revealed significant changes in 2 metabolic pathways, valine, leucine, isoleucine biosynthesis, and nitrogen metabolism in the L-GLY, H-GLY, HFD, L-GLY+HFD, and H-GLY+HFD treatment groups compared to the Ctrl group. Neomycin, kanamycin, and gentamicin biosynthesis were also significantly changed after exposure to HFD and H-GLY+HFD. The top 5 disrupted metabolic pathways in each treatment group included glyoxylate and dicarboxylate metabolism, glycine, serine, and threonine metabolism, and alanine, aspartate, and glutamate metabolism (Table S4).

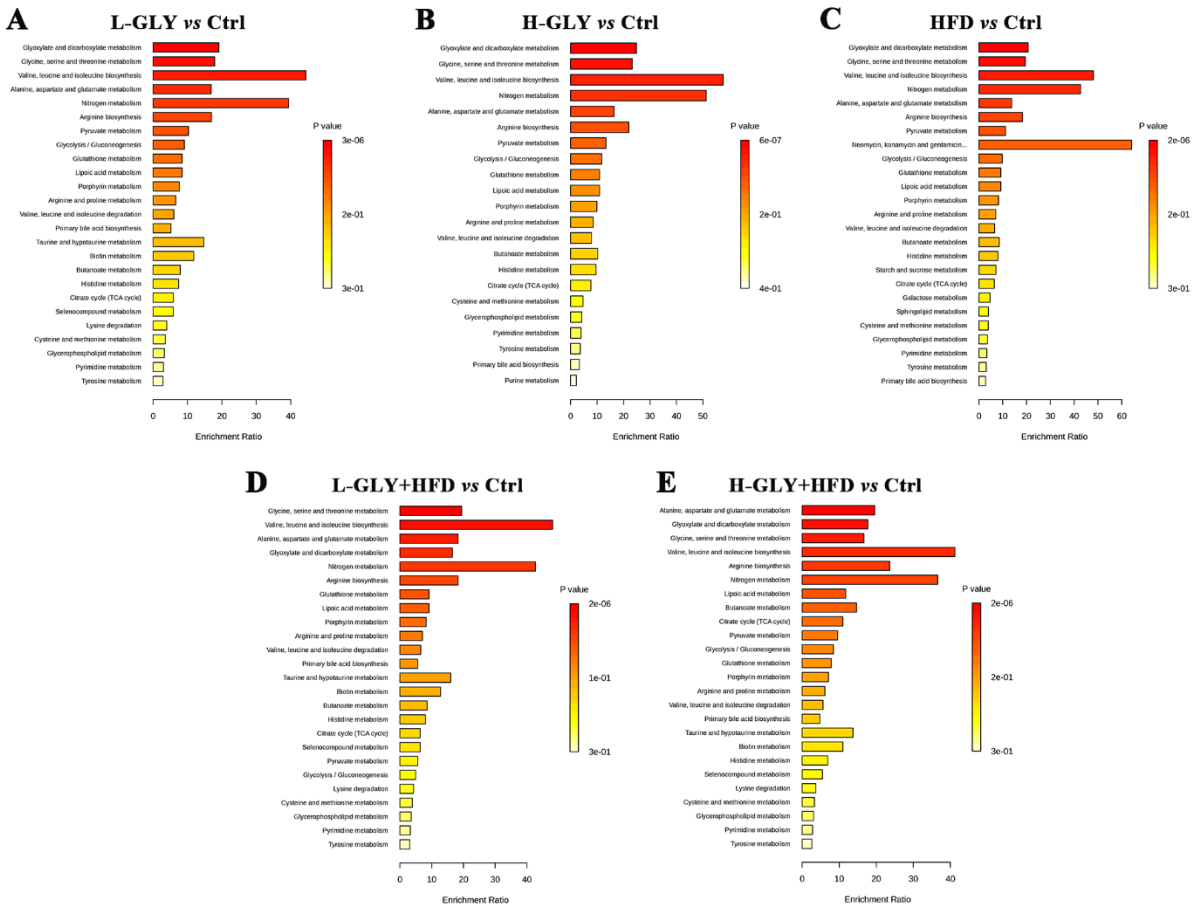

Fig. 4. The significantly disturbed metabolic pathways identified from pathway analysis using the web service of MetaboAnalyst 5.0. (A) L-GLY vs Ctrl, (B) H-GLY vs Ctrl, (C) HFD vs Ctrl, (D) L-GLY+HFD vs Ctrl, (E) H-GLY+HFD vs Ctrl.

3.4 GLY disrupted liver lipid homeostasis of zebrafish under different dietary conditions

Metabolomics analysis revealed changes in the levels of energy metabolism-related metabolites in zebrafish liver after exposure to L-GLY, H-GLY, HFD, L-GLY+HFD, and H-GLY+HFD. The underlying molecular mechanisms were explored by quantifying the mRNA expression levels of several genes involved in lipid metabolism using qRT-PCR (Fig. 5A). Notably, there was significant upregulation of mRNA expression levels of genes associated with fatty acid biosynthesis (*Fasn*, *Acaca*, *Fabp10a*, *Hmgcra*, *Lpl*, and *Fat*) in zebrafish liver. Noteworthy, the mRNA expression level of *Fasn* was significantly upregulated after exposure to L-GLY+HFD and H-GLY+HFD compared to the Ctrl group (F=17.49, $P < 0.001$). The expression level of *Fasn* was also significantly upregulated in the H-GLY+HFD treatment group compared to the HFD group (F=17.49, $P < 0.001$). There was a significant increase in the expression levels of *Acaca* in the L-GLY, H-GLY, L-GLY+HFD, and H-GLY+HFD treatment groups (F=17.52, $P < 0.001$). Moreover, there was a significant increase in the expression levels of *Acaca* and *Fabp10a* in the L-GLY+HFD and H-GLY+HFD treatment groups compared to the HFD treatment group (F=17.52, $P < 0.001$ for *Acaca*, F=6.825,$P < 0.001$ for *Fabp10a*). Exposure to H-GLY, HFD, L-GLY+HFD, and H-GLY+HFD significantly increased the expression level of *Lpl* (F=19.31, $P < 0.001$). Similarly, the expression level of *Fat* significantly increased after exposure to L-GLY+HFD and H-GLY+HFD compared to the Ctrl group (F=10.170, $P <$

0.001). The expression level of *Fat* also significantly increased after exposure to H-GLY+HFD compared to the HFD treatment group (F=10.170, $P < 0.001$) (Fig. 5B). In contrast, there was a significant decrease in the expression level of *Cpt1a* in the L-GLY, H-GLY, and H-GLY+HFD treatment groups compared to the Ctrl group (F=6.701, $P < 0.001$). The expression level of *Pgcla* was also significantly downregulated in the L-GLY, H-GLY, L-GLY+HFD, and H-GLY+HFD treatment groups compared to the Ctrl group (F=11.570, $P < 0.001$) (Fig. 5C). Moreover, the mRNA expression levels of nuclear hormone receptor genes (*Pparg*, *Pparaa*, and *Pparab*) were also determined. *Pparg* was significantly increased in the H-GLY, HFD, L-GLY+HFD and H-GLY+HFD treatment groups. The expression level of *Pparg* was also significantly increased after exposure to L-GLY+HFD and H-GLY+HFD compared to the HFD treatment group (F=11.380, $P < 0.001$). The expression levels of *Pparaa* and *Pparab* were significantly upregulated in the HFD treatment group compared to the Ctrl group. Exposure to L-GLY and H-GLY significantly reduced the expression levels of *Pparaa* and *Pparab* activated by HFD (F=1.631, p=0.020 for *Pparaa*, F=5.036, p=0.002 for *Pparab*) (Fig. 5D).

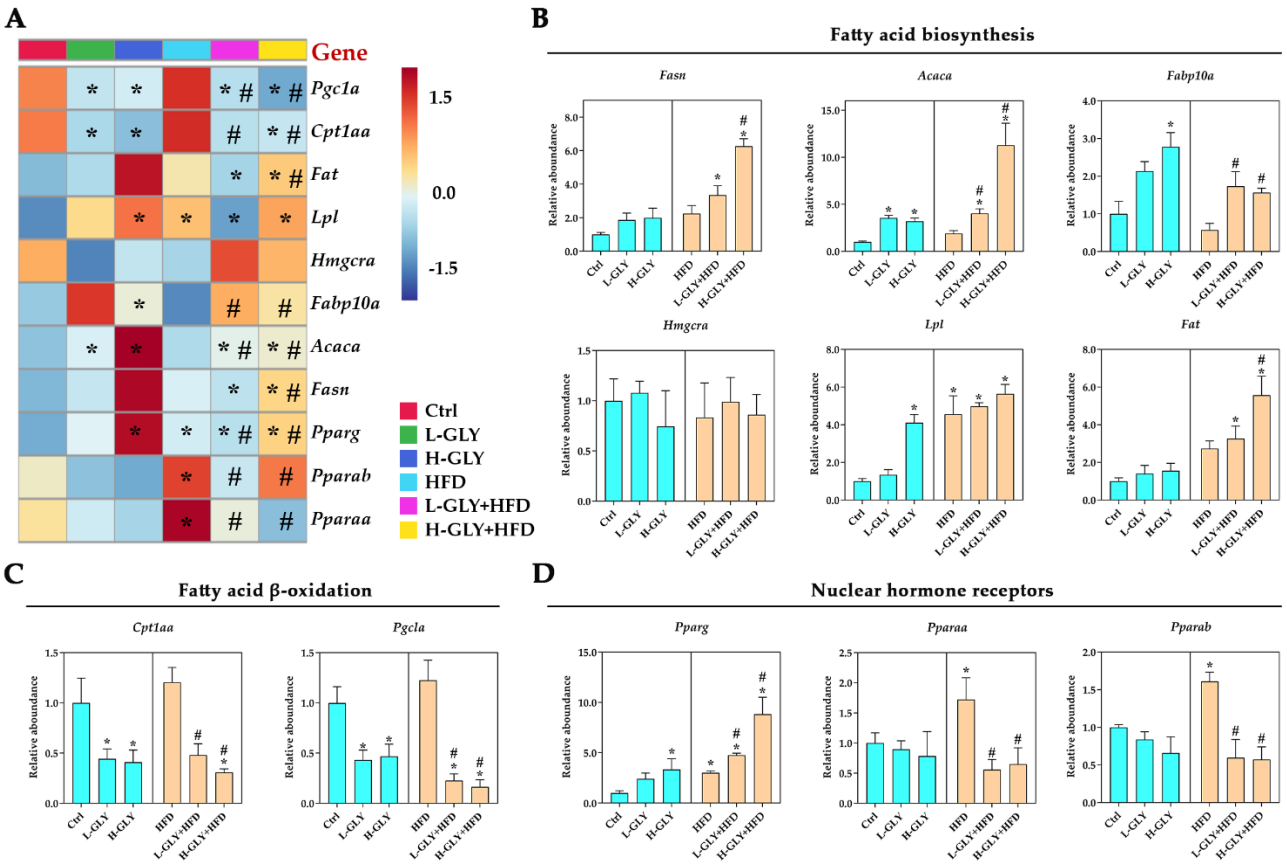

Fig. 5. Exposure to GLY disrupted lipid homeostasis in liver of zebrafish. (A) Heat map of the relative changes in mRNA expression of lipid metabolism-related genes in liver tissue of zebrafish, (B) The mRNA expressions levels of fatty acid biosynthesis related genes, (C) The mRNA expressions levels of fatty acid oxidation related genes, (D) The mRNA expressions levels of nuclear hormone receptors related genes. Data are expressed as mean ± SD. $^{*}P < 0.05$ compared with the Ctrl treatment group. $^{\#}P < 0.05$ compared with the HFD treatment group.

Note: *Fasn*: Fatty acid synthase, *Acaca:* Acetyl-CoA carboxylase, *Fabp10a*: Fatty acid-binding protein 10a , *Hmgcra*: Recombinant 3-hydroxy-3-methylglutaryl coenzyme a reductase a, *Lpl*: lipoprotein lipase, *Fat*: Fatty acid translocase, Cpt1aa: Carnitine palmitoyltransferase 1aa, *Pgc1a*: Peroxisome proliferator-activated receptor γ coactivator 1a, *Pparg*: Peroxisome proliferative activated receptor gamma, *Pparaa*: Peroxisome proliferator-activated receptor alpha a, *Pparab*: *Peroxisome* proliferator-activated receptor alpha b.

3.5 GLY disrupts the intestinal function of zebrafish under different dietary conditions

The host's liver function is closely associated with intestinal homeostasis. The effects of GLY on the intestinal function of zebrafish under different dietary conditions were thus investigated further. Colonic H&E staining revealed significant structural damage and infiltration of inflammatory cells in the intestinal tissue after exposure of zebrafish to L-GLY, H-GLY, HFD, L-GLY+HFD, and H-GLY+HFD (Fig. 6A). Notably, there was a significant reduction in the villus height and crypt depth of the intestine of zebrafish in the L-GLY, H-GLY, HFD, L-GLY+HFD and H-GLY+HFD treatment groups. The villus height and crypt depth of the intestine of zebrafish exposed to L-GLY+HFD and H-GLY+HFD were also significantly reduced compared to those in the HFD treatment group (F=100.2, $P < 0.001$ for villus height, F=44.28, $P < 0.001$ for crypt depth) (Fig. 6B and C). The expression levels of mucin secretion-related genes of *Mucin2* and *Claudin10* were significantly inhibited after exposure to L-GLY, H-GLY, L-GLY+HFD, and H-GLY+HFD compared to the Ctrl group. Similarly, the expression levels of *Mucin2* and *Claudin10* were significantly reduced in the L-GLY+HFD and H-GLY+HFD treatment groups compared to the HFD treatment group (F=4.417, p=0.004 for *Mucin2*, F=17.77, $P < 0.001$ for *Claudin10*)(Fig. 6D and F). The expression level of *Zo 1* in the H-GLY+HFD treatment group was significantly reduced compared to the corresponding expression in the Ctrl and HFD treatment groups (F=1.867, p=0.130) (Fig. 6E). There was a significant increase in the expression level of *Tnfα* after zebrafish exposure to L-GLY, H-GLY, HFD, L-GLY+HFD, and H-GLY+HFD compared to the Ctrl group (F=26.00, $P < 0.001$) (Fig. 6G). *Il1β* and *Cxcl18β* were significantly upregulated in the H-GLY and H-GLY+HFD treatment groups compared to the Ctrl group (F=20.66, $P < 0.001$ for *Il1β*, F=8.766, $P < 0.001$ for *Cxcl18β*) (Fig. 6H and I). Notably, exposure to H-GLY+HFD resulted in significant upregulation of *Tnfα*, *Il1β*, and *Cxcl18β* compared to the HFD treatment group (Fig. 6G, H, and I).

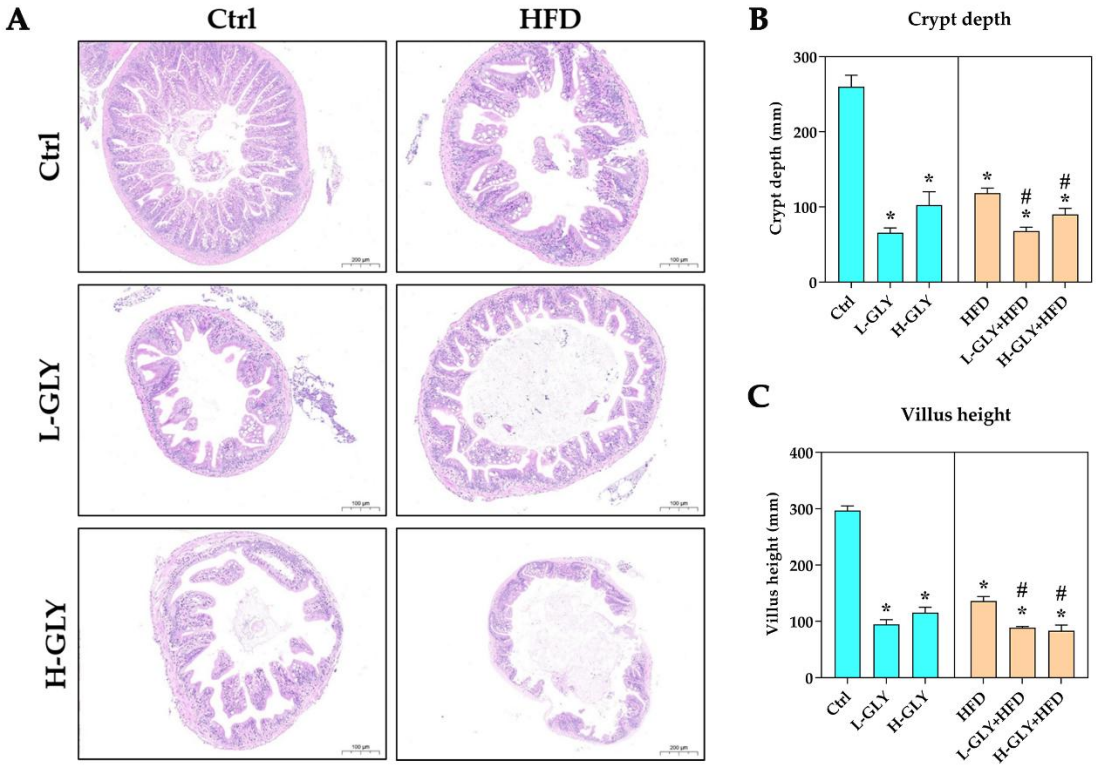

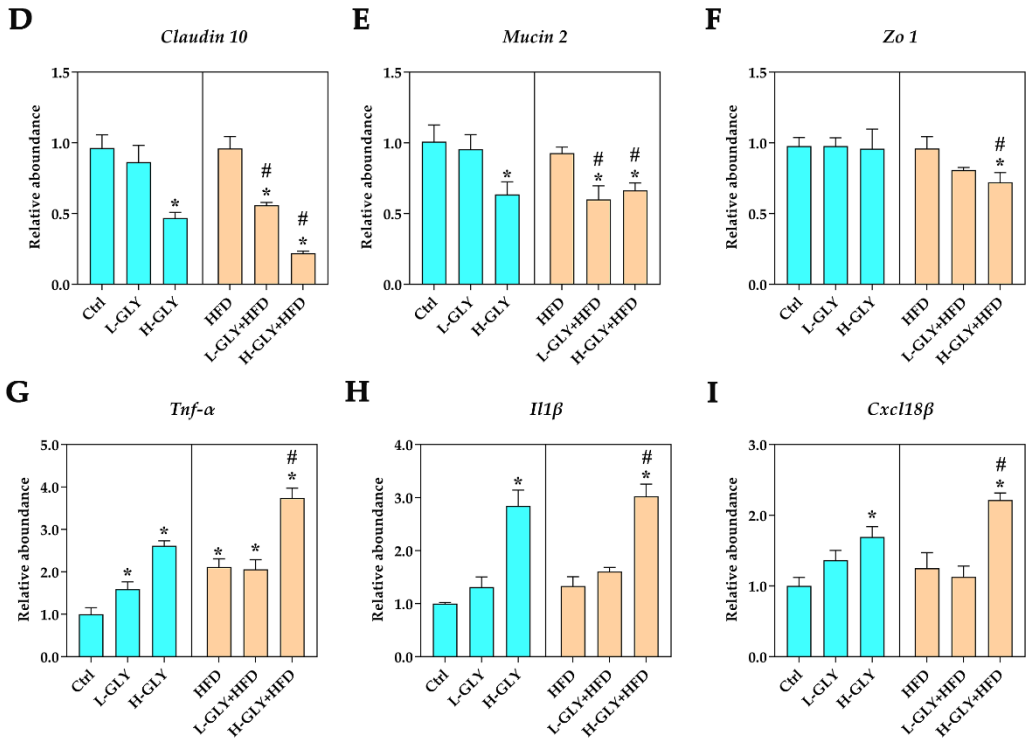

Fig. 6. Exposure to GLY disrupts intestinal function of zebrafish. (A) Representative images of H&E staining of intestinal tissues, (B) Villus height of intestinal tissues, (C) Crypt depth of intestinal tissues, (D-F) The m RNA expression levels of tight junction protein related genes, (E-F) The m RNA expression levels of inflammatory cytokine related genes. Data are expressed as mean ± SD. *$P < 0.05$ compared with the Ctrl treatment group. $^{\#}P < 0.05$ compared with the HFD treatment group.

3.6 GLY exposure induced dysbiosis of gut microbiota in zebrafish under different dietary conditions

The effects of GLY on the structure and function of gut microbiota were evaluated under different dietary conditions. The β-diversity of the gut microbiota was assessed using the principal component analysis (PCA) score plot. The PCA score plot clearly distinguished between the 5 treatment groups and the Ctrl group. This phenomenon suggested that exposure to L-GLY, H-GLY, HFD, L-GLY+HFD, and H-GLY+HFD significantly affected the gut microbiome of zebrafish (Fig.7A). Moreover, changes in the α-diversity indexes, Chao1, Simpson, Observed_species, and Shannon were evaluated. L-GLY+HFD significantly increased the value of Observed_species compared to the Ctrl group (Fig.7B). Analysis of changes in gut microbiota composition in zebrafish at phylum and genus levels (Fig.7C and F) revealed a significant increase in the relative abundance of *Firmicutes* in the L-GLY, H-GLY, L-GLY+HFD, and H-GLY+HFD treatment groups compared to the Ctrl group at the phylum level. In contrast, there was a significant decrease in the relative abundances of *Bacteroidetes* and *Spirochaetes* in these treatment groups compared to the Ctrl group (Fig.7D). The relative abundance of *Tenericutes* also underwent significant changes after exposure to L-GLY, H-GLY, and HFD. H-GLY+HFD exposure led to a significant increase in the relative abundance of *Verrucomicrobia* (Fig.7D). There was a significant decrease in the relative abundance of *Bacteroidetes* in the L-GLY+HFD treatment group compared to the HFD treatment group. In contrast, there was a significant increase in the relative abundance of *Verrucomicrobia* in the H-GLY+HFD treatment group compared to the HFD treatment group. The relative abundance of *Spirochaetes* significantly decreased in the L-GLY+HFD and H-GLY+HFD

treatment groups compared to the HFD treatment group (Fig.7D). Notably, the ratio of the relative abundances of *Firmicutes* to *Bacteroidetes* significantly increased in the L-GLY, H-GLY, L-GLY+HFD, and H-GLY+HFD treatment groups compared to the Ctrl group. There was a significant increase in the ratio of *Firmicutes* to *Bacteroidetes* in the L-GLY+HFD treatment group compared to the HFD treatment group (Fig.7E). The relative abundance of *Lactobacillus* significantly increased while that of *Prevotella* and *Corynebacterium* significantly decreased in the L-GLY, H-GLY, HFD, L-GLY+HFD, and H-GLY+HFD treatment groups compared to the Ctrl group at the genus level (Fig.7G). Moreover, exposure of zebrafish to L-GLY, H-GLY, L-GLY+HFD, and H-GLY+HFD resulted in significant decreases in the relative abundances of *Staphylococcus* and *Treponema* compared to the Ctrl group (Fig.7G). The relative abundances of *Staphylococcus* and *Treponema* were significantly reduced in the L-GLY+HFD and H-GLY+HFD treatment groups compared to the HFD treatment group. Zebrafish exposure to H-GLY+HFD also led to significant increases in the relative abundances of *Corynebacterium* and *Hyphomicrobium*, and a significant decrease in the relative abundance of *Roseburia* (Fig.7G).

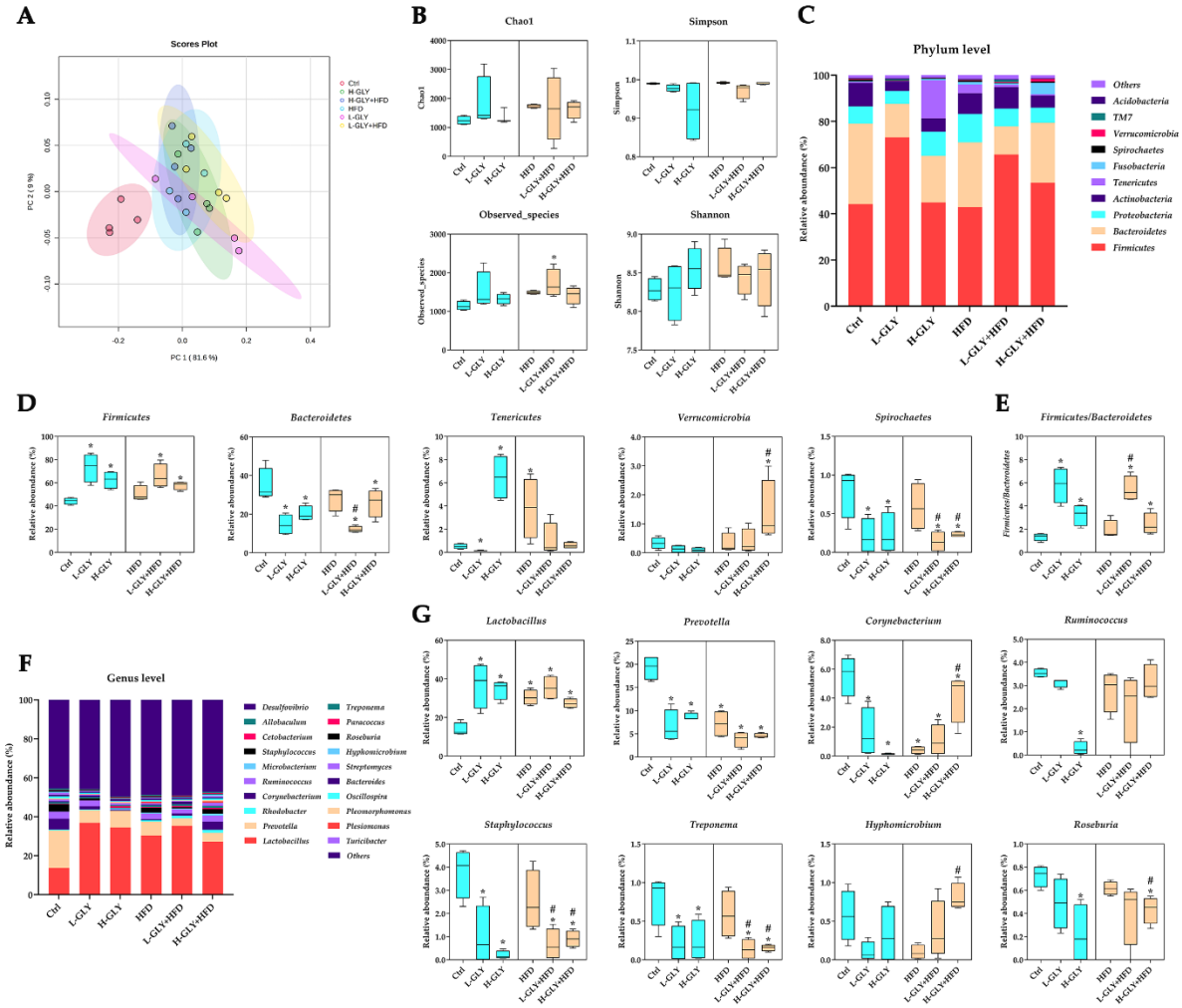

Fig. 7. Exposure to GLY induced gut microbiota dysbiosis of zebrafish. (A) PCA score plot of gut microbiota based on OUT abundance, (B) α-diversity indexes, (C) Average relative abundances of gut microbiota at the phylum level, (D) Relative abundances of the representative bacteria that significantly changed at the phylum level, (E) Ratio of the relative abundances of *Firmicutes* and *Bacteroidetes*, (F) Average relative abundances of gut microbiota at the genus level, (D) Relative abundances of the representative bacteria that significantly changed at the genus level. Data are expressed as mean ±SD. $^{*}P < 0.05$ compared with the Ctrl treatment group. $^{\#}P < 0.05$ compared with the HFD treatment group.

4. Discussion

Glyphosate (GLY) is a popular herbicide that is widely used, often remaining in various media, such as soil, water, and plants, thereby posing significant potential risks to the ecological environment and human health [26, 27]. Herein, zebrafish were used as a model organism to investigate the effects of different doses of GLY (0, 50, and 500 μg/L) and different dietary conditions (6% crude fat and 24% crude fat) on liver function. In this study, we provide new insights into the effects of GLY on liver function, intestinal barrier function, and gut microbiota composition of zebrafish under different dietary conditions.

GLY significantly increased the body weight and length of zebrafish. High GLY doses caused more pronounced changes than low GLY doses. Notably, GLY caused an increase in the body weight and length of zebrafish under HFD. All GLY treatment groups exhibited hepatic lipid degeneration and inflammatory responses. The adverse effects of GLY on the liver were further amplified under HFD. *Tnfα* and *Il1β* are the main pro-inflammatory cytokines that induce inflammatory response processes and are closely associated with metabolic dysfunction [28]. Herein, metabolomics analysis revealed that exposure to GLY significantly altered the metabolic phenotypes of the liver, causing notable changes in the levels of metabolites associated with energy metabolism. Combined GLY and HFD treatment resulted in changes in the levels of more metabolites. Correlation analysis revealed a significant correlation between changes in the content of glutamate and glutamine and changes in the TC content (Fig.8B). Glutamine is the most abundant free amino acid in the body and can be hydrolyzed into glutamate through phosphate-dependent glutaminase. Gutamate can be subsequently converted into metabolites, such as a-ketoglutarate, aspartic acid, pyruvic acid, and lactic acid [29, 30]. These metabolites can be thoroughly oxidized and decomposed, thereby regulating lipid and glucose metabolism in the body [31]. Moreover, there was a significant positive correlation between the changes in leucine and alanine content and changes in TC content (Fig.8B). Leucine is a branched-chain amino acid that regulates mitochondrial dysfunction and affects lipid metabolism in the body[32]. Alanine participates in the metabolism of proteins, fats, and carbohydrates, thereby regulating cholesterol levels in the liver [33]. An investigation of the liver lipid imbalance induced by GLY under different dietary conditions at the genetic level (Fig.8C) revealed a significant increase in the expression level of *Acaca* attributed to GLY exposure. *Acaca* is a crucial gene that regulates fatty acid biosynthesis. Its upregulation implies that GLY promotes fatty acid synthesis [34]. *Cpt1aa* and *Pgc1a*, which play important roles in fatty acid oxidation, were significantly downregulated after GLY exposure [35,36]. This phenomenon suggested that GLY also significantly inhibits the metabolism of fatty acids. Similarly, GLY significantly increased the expression levels of *Fasn*, *Fabp10a*, and *Fat* under HFD. *Fasn*, *Fabp10a*, and *Fat* play vital regulatory roles in regulating fatty acid synthesis [37]. These results further confirmed that GLY can promote fatty acid synthesis under different dietary conditions. Moreover, GLY led to upregulation of the expression level of *Pparg* and downregulation of the expression levels of *Pparaa* and *Pparab*. *Pparg* is a crucial transcription factor that regulates lipid metabolism by stimulating the expression of genes involved in lipid synthesis [38]. *Pparaa* and *Pparab* also regulate the expression of genes associated with fatty acid breakdown

[39]. Importantly, PPARα is a central signaling pathway that regulates hepatic fatty acid β-oxidation and lipid homeostasis [40]. In this study, we found that GLY impairs its normal function by directly or indirectly inhibiting the transcriptional activity of PPARα. This inhibition disrupts the balance between fatty acid uptake, synthesis, and catabolism in the liver, leading to the abnormal accumulation of lipids that cannot be efficiently oxidized, thereby contributing to hepatic steatosis. Furthermore, lipid accumulation can promote inflammatory responses, which may ultimately cause hepatocyte damage and mediate the hepatotoxicity of GLY. In short, these results collectively suggested that GLY-induced lipid accumulation in the liver of zebrafish under different dietary conditions is potentially associated with the PPAR signaling pathway.

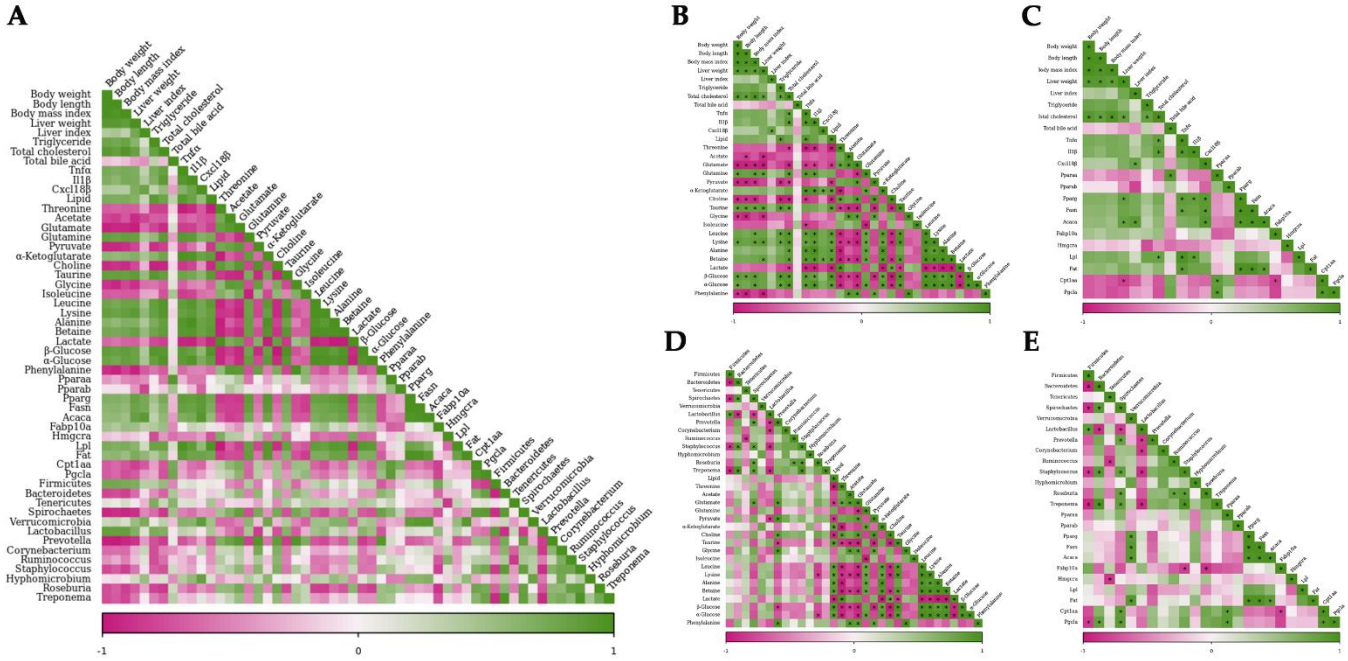

Fig. 8. Pearson correlation analysis to clarify the relationship based toxicity effects of zebrafish induced by GLY. (A) Pearson correlation analysis to clarify the relationship between liver damage, liver metabolic profile disorders, liver lipid metabolism imbalances and gut microbiota dysbiosis, (B) Pearson correlation analysis to clarify the relationship between liver damage and liver metabolic profile disorders, (C) Pearson correlation analysis to clarify the relationship between liver damage and liver lipid metabolism imbalances, (D) Pearson correlation analysis to clarify the relationship between liver metabolic profile disorders and gut microbiota dysbiosis, (E) Pearson correlation analysis to clarify the relationship between liver lipid metabolism imbalances and gut microbiota dysbiosis.

In recent years, an increasing number of studies have postulated that the gut microbiota is closely associated with the liver function of organisms. This association is through the “gut-liver axis” [41]. The intestinal barrier is an important structural element of the gut-liver axis, which serves as a functional and physical barrier between the gut microbiota and the liver tissue [42, 43]. Recent studies postulate that exposure to pesticides, such as tebuconazole and azoxystrobin, significantly affects the functioning of the biological intestinal barrier and could lead to colitis in organisms in some cases [44,45]. Herein, GLY disrupted the intestinal structure and function of zebrafish, leading to significant changes in intestinal inflammation and barrier-related genes. The 16sRNA sequencing results revealed significant changes in the composition and structure of gut microbiota after GLY exposure under different dietary conditions. There was a significant change in the relative content of *Firmicutes* and *Bacteroidetes* at the phylum level. The ratio of *Firmicutes* to *Bacteroidetes* significantly increased after GLY exposure. *Firmicutes* and *Bacteroidetes* are closely

associated with energy metabolism in organisms. An increase in the ratio of *Firmicutes* to *Bacteroidetes* is often associated with obesity in organisms [46, 47]. A recent study postulated that exposure to the fungicide chlorothalonil increased the ratio of *Firmicutes* to *Bacteroidetes* in mice, thereby promoting lipid accumulation in the liver [48]. In this study, there was a significant correlation between the relative abundance of *Prevotella* and the levels of liver metabolites, glutamate, pyruvate, choline, taurine, and glycine (Fig.8D). A decrease in *Prevotella* abundance is not conducive to the breakdown of proteins and carbohydrates because it is closely associated with dietary conditions [49, 50]. Moreover, there was a significant correlation between the relative abundances of *Verrucomicobia* and the expression levels of fatty acid synthesis related genes (*Pparg*, *Fasn*, *Acaca*, and *Fat*) (Fig.8E). The relative abundance of *Spirochaetes* was significantly correlated with the expression of fatty acid oxidation genes (*Cpt1aa* and *Pgc1a*) (Fig.8E). This discovery suggests that the changes in gut microbiota caused by GLY exposure are closely associated with liver lipid accumulation.

Notably, the adverse effects of GLY on zebrafish were further exacerbated under HFD. We found that combined treatment of GLY and HFD could disrupt the integrity of the intestinal barrier and cause an upregulation of inflammatory cytokine levels. Meanwhile, it could significantly alter the structure of gut microbiota, causing metabolic profile disorders in the zebrafish. These factors collectively increase the burden on the liver, inhibit lipid metabolism, promote fat accumulation, and trigger inflammatory reactions, ultimately leading to liver cell damage. Unfortunately, while we have identified the interactive effects of GLY and HFD on the gut-liver axis, the crucial role of the gut microbiota in this process still requires further validation. Moreover, it remains essential to determine which specific microbial communities are responsible for regulating the induction of liver toxicity by GLY and HFD.

5. Conclusion

GLY exposure promotes liver lipid accumulation, leading to structural damage and an inflammatory response of the liver. Notably, GLY exacerbated liver lipid accumulation under HFD. GLY exposure led to metabolic disorders in the liver of zebrafish under different dietary conditions, causing significant changes in the contents of metabolites associated with energy metabolism. GLY exposure also significantly changed the expression levels of genes associated with fatty acid synthesis and oxidation in the liver tissue of zebrafish. Moreover, GLY exposure damaged the intestinal barrier function and disrupted the gut microbiota under different dietary conditions. Notably, the changes in gut microbiota composition caused by GLY exposure were closely associated with liver lipid accumulation. The toxicity effects involving liver and intestinal function of zebrafish under the combined action of GLY and HFD were more severe. The findings of this study suggest that the gut-liver axis can potentially regulate the hepatotoxicity of GLY and highlight the dynamics of the environmental health risks of pesticides under different dietary conditions.

Declaration of competing interest

The authors declare that they have no known competing financial interests or personal relationships that could have appeared to influence the work reported in this paper.

Acknowledgments

We gratefully acknowledge the financial support received from the National Natural Science Foundation of China (42407375), the Natural Science Foundation of Jiangsu Province (BK20240903), the Natural Science Foundation of the Jiangsu Higher Education Institutions of China (24KJD610006) and the Science and Technology Projects Fund of Yangzhou City (YZ2024074).

Reference

[1] S.R. Liu, R. Jia, J.Y. Zhu, et al., Integrated physiological, metabolite and proteomic analysis reveal the glyphosate stress response mechanism in tea plant (*Camellia sinensis*). J. Hazard. Mater. 454 (2023) 131419. https://doi.org/10.1016/j.jhazmat.2023.131419.

[2] R. Lacroix, D.M. Kurrasch, Glyphosate toxicity: in vivo, in vitro, and epidemiological evidence. Toxicol. Sci. 192 (2023) 131-140.https://doi.org/10.1093/toxsci/kfad018.

[3] F. Sun, L. Yang, S.J. Li, et al., New fluorescent probes for the sensitive determination of glyphosate in food and environmental samples. J. Agric. Food Chem. 69 (2021) 12661–12673. https://doi.org/10.1021/acs.jafc.1c05246.

[4] Y. Geng, L.J. Jiang, D.Y. Zhang, et al., Glyphosate, aminomethylphosphonic acid, and glufosinate ammonium in agricultural groundwater and surface water in China from 2017 to 2018: Occurrence, main drivers, and environmental risk assessment. Sci. Total Environ. 769 (2021) 144396. https://doi.org/10.1016/j.scitotenv.2020.144396

[5] M.R. Jan, J. Shah, M. Muhammad, et al., Glyphosate herbicide residue determination in samples of environmental importance using spectrophotometric method. J. Hazard. Mater. 169 (2009) 742-745. https://doi.org/10.1016/j.jhazmat.2009.04.003.

[6] J.L. Vicini, P.K. Jensen, B.M. Young, et al., Residues of glyphosate in food and dietary exposure. Compr. Rev. Food Sci. Food Saf. 20 (2021) 5226-5257. https://doi.org/10.1111/1541-4337.12822.

[7] J. Lu, W.G. Wang, C. Zhang, et al., Characterization of glyphosate-induced cardiovascular toxicity and apoptosis in zebrafish. Sci. Total Environ. 851 (2022) 108308. https://doi.org/10.1016/j.scitotenv.2022.158308.

[8] R. Leoci, M. Ruberti, Glyphosate in agriculture: environmental persistence and effects on animals. A Review. J. Agric. Environ. Int. 114 (2020) 99-123. https://doi.org/10.12895/jaeid.20201.1167.

[9] P.C. Lehman, N. Cady, S. Ghimire, et al., Low-dose glyphosate exposure alters gut microbiota composition and modulates gut homeostasis. Environ. Toxicol. Pharmacol. 100 (2023) 104149. https://doi.org/10.1016/j.etap.2023.104149.

[10] R. Mesnage, A. Phedonos, M. Biserni, et al., Evaluation of estrogen receptor alpha activation by glyphosate-based herbicide constituents. Food Chem. Toxicol. 108 (2017) 30-42. https://doi.org/10.1016/j.fct.2017.07.025.

[11] M.G. Schimpf, M.M. Milesi, M.V. Zanardi, et al., Disruption of developmental programming with long-term consequences after exposure to a glyphosate-based herbicide in a rat model. Food Chem. Toxicol. 159 (2022) 112695. https://doi.org/10.1016/j.fct.2021.112695.

[12] X. Ren, P.Y. Dai, A. Perveen, et al., Effects of chronic glyphosate exposure to pregnant mice on hepatic lipid metabolism in offspring. Environ. Pollut. 254. (2019) 112906. https://doi.org/10.1016/j.envpol.2019.07.074.

[13] J. Chavez-Reyes, C.D. Gutierrez-Reyes, E. Hernandez-Cuellar, et al., Neurotoxicity of glyphosate: Focus on molecular mechanisms probably associated with alterations in cognition and behavior. Environ. Toxicol. Pharmacol. 106 (2024) 104381. https://doi.org/10.1016/j.etap.2024.104381.

[14] M. Kobayashi, T. Ohno, T. Tsuchiya, et al., Characterization of diabetes-related traits in MSM and JF1 mice on high-fat diet. J. Nutr. Biochem. 15 (2004) 614-621. https://doi.org/10.1016/j.jnutbio.2004.05.001.

[15] Y. Wan, F.L. Wang, J.H. Yuan, et al., Effects of dietary fat on gut microbiota and faecal metabolites, and their relationship with cardiometabolic risk factors: a 6-month randomised controlled-feeding trial. Gut 68 (2019) 1417-+. https://doi.org/10.1136/gutjnl-2018-317609.

[16] J.L. Chen, Y.H. Xiao, D.M. Li, et al., New insights into the mechanisms of high-fat diet mediated gut microbiota in chronic diseases. Imeta 2(2023) e69. https://doi.org/10.1002/imt2.69.

[17] X. Li, J.D. Zhang, H. Xiao, et al., Triclocarban and triclosan exacerbate high-fat diet-induced hepatic lipid accumulation at environmental related levels: The potential roles of estrogen-related receptors pathways. Sci. Total Environ. 858 (2023) 160079. https://doi.org/10.1016/j.scitotenv.2022.160079.

[18] J.W. Li, X.D. Li, Z.H. Zhang, et al., High-fat diet aggravates the disorder of glucose metabolism caused by chlorpyrifos exposure in experimental rats. Foods 12 (2023) 816. https://doi.org/10.3390/foods12040816.

[19] J.Y. Wu, K. Wang, X.M. Wang, et al., The role of the gut microbiome and its metabolites in metabolic diseases. Proteins Cell Regul. 12 (2021) 360-373. https://doi.org/10.1007/s13238-020-00814-7.

[20] J. Liu, X.Y. Yuan, C.X. Fan, et al., Application of the zebrafish model in human viral research. Virus Res. 341 (2024) 199327. https://doi.org/10.1016/j.virusres.2024.199327.

[21] N. Djekkoun, F. Depeint, M. Guibourdenche, et al., Perigestational exposure of a combination of a high-fat diet and pesticide impacts the metabolic and microbiotic status of dams and pups; a preventive strategy based on prebiotics. Eur. J. Nutr. 62 (2023) 1253-1265. https://doi.org/10.1007/s00394-022-03063-y.

[22] Y.H. Wang, Z. Kuang, X.F. Yu, et al., The intestinal microbiota regulates body composition through NFIL3 and the circadian clock. Science 357 (2017) 913-+. https://doi.org/10.1126/science.aan0677.

[23] E.M. Brovini, S.J. Cardoso, G.R. Quadra, et al., Glyphosate concentrations in global freshwaters: are aquatic organisms at risk? Environ. Sci. Pollut. Res. 28 (2020) 60635-60648. https://doi.org/10.1007/s11356-021-14609-8.

[24] J.P. Muñoz, E.Silva-Pavez, D. Carrillo-Beltrán, et al., Occurrence and exposure assessment of glyphosate in the environment and its impact on human beings. Environ. Res. 231 (2023) 116201. https://doi.org/10.1016/j.envres.2023.116201.

[25] Z.Y. Meng, J.J. Cui, L. Liu, et al., Toxicity effects of chlorantraniliprole in zebrafish (*Danio rerio*) involving in liver function and metabolic phenotype. Pestic. Biochem. Physiol. 187 (2022) 105194. https://doi.org/10.1016/j.pestbp.2022.105194.

[26] C.R. Hentges, L.K. Schuck, C.D.A. Caberlon, et al., Impact of environmentally relevant concentrations of glyphosate on boana faber tadpoles exposed in the laboratory: morphological and functional markers. Environ. Toxicol. Pharmacol. 114 (2025) 104643. https://doi.org/10.1016/j.etap.2025.104643.

[27] L. Hu, M.C. Chen, X.R. Xue, et al., Effect of glyphosate on renal function: A study integrating epidemiological and experimental evidence. Ecotoxicol. Environ. Saf. 290 (2025) 117758. https://doi.org/10.1016/j.ecoenv.2025.117758.

[28] P.J. Gaglio, Nonalcoholic fatty liver disease preface. Clin. Liver. Dis. 20 (2016) XIII-XIV. https://doi.org/10.1016/j.cld.2016.02.001.

[29] B.J. Deters, M. Saleem, The role of glutamine in supporting gut health and neuropsychiatric factors. Food Sci. Hum. Wellness 10 (2021) 149-154. https://doi.org/10.1016/j.fshw.2021.02.003.

[30] P. Yuliandari, I.P.B. Mayura, Effect of helicobacter pylori infection on glucose metabolism, lipid metabolism and inflammatory cytokines in nonalcoholic fatty liver disease patients. J. Multidiscip. Healthc. 17 (2024) 1413-1414. https://doi.org/10.2147/jmdh.S469382.

[31] H.M. German, J. Ciapaite, N.M. Verhoeven-Duif, et al., Anaplerosis by medium-chain fatty acids through complex interplay with glucose and glutamine metabolism. J. Biol. Chem. (2025) 108307. https://doi.org/10.1016/j.jbc.2025.108307.

[32] M.Z. Farooq, A.R. Ansari, Transcriptomic analysis reveals the effect of leucine deprivations and starvation on glucose and lipid metabolism on mice liver. Gene Rep. 38 (2025) 102134. https://doi.org/10.1016/j.genrep.2025.102134.

[33] J.H. Jeong, S. Jung, K.N. Kim, et al., Considering serum alanine aminotransferase and gamma-glutamyltransferase levels together strengthen the prediction of impaired fasting glucose risk: a cross-sectional and longitudinal study. Sci. Rep. 11 (2021) 11346. https://doi.org/10.1038/s41598-021-82981-z.

[34] J.E. Cronan, G.L. Waldrop, Multi-subunit acetyl-CoA carboxylases. Prog. Lipid Res. 41 (2002) 407-435. https://doi.org/10.1016/s0163-7827(02)00007-3.

[35] K. Bhalla, B.J. Hwang, R.E. Dewi, et al., PGC1α promotes tumor growth by inducing gene expression programs supporting lipogenesis. Cancer Res. 71 (2011) 6888-6898. https://doi.org/10.1158/0008-5472.Can-11-1011.

[36] D.O. Espinoza, L.G. Boros, S. Crunkhorn, et al., Dual modulation of both lipid oxidation and synthesis by peroxisome proliferator-activated receptor-γ coactivator-1α and-1β in cultured myotubes. Faseb J. 24 (2010) 1003-1014. https://doi.org/10.1096/fj.09-133728.

[37] W. Guo, L. Lei, X.J. Shi, et al., Nonalcoholic fatty liver disease development in zebrafish upon exposure to bis(2-ethylhexyl)-2,3,4,5-tetrabromophthalate, a novel brominated flame retardant. Environ. Sci. Technol. 55 (2021) 6926-6935. https://doi.org/10.1021/acs.est.1c01476.

[38] R.M. Evans, G.D. Barish, Y.X. Wang, PPARs and the complex journey to obesity. Nat. Med. 10 (2004) 355-361. https://doi.org/10.1038/nm1025.

[39] M. Inoue, T. Ohtake, W. Motomura, et al., Increased expression of PPARγ in high fat diet-induced liver steatosis in mice. Biochem. Biophys. Res. Commun. 336 (2005) 215-222. https://doi.org/10.1016/j.bbrc.2005.08.070.

[40] X. Yang, Y.J. Fu, F.Q. Hu, et al., PIK3R3 regulates PPARα expression to stimulate fatty acid β-oxidation and decrease hepatosteatosis. Exp. Mol. Med. 50 (2018) e431. https://doi.org/10.1038/emm.2017.243.

[41] C.L. Hsu, B. Schnabl, The gut-liver axis and gut microbiota in health and liver disease. Nat. Rev. Microbiol. 21 (2023) 719-733. https://doi.org/10.1038/s41579-023-00904-3.

[42] O. Pabst, M.W. Hornef, F.G. Schaap, et al., Gut-liver axis: barriers and functional circuits. Nat. rev. gastroenterol. hepatol. 20 (2023) 447-461. https://doi.org/10.1038/s41575-023-00771-6.

[43] Z.P. Zheng, B.H. Wang, The gut-liver axis in health and disease: the role of gut microbiota-derived signals in liver injury and regeneration. Front. Immunol. 12 (2021) 775526. https://doi.org/10.3389/fimmu.2021.775526.

[44] Z.Y. Meng, W. Sun, W. Liu, et al., A common fungicide tebuconazole promotes colitis in mice via regulating gut microbiota. Environ. Pollut. 292 (2022) 118477. https://doi.org/10.1016/j.envpol.2021.118477.

[45] Z.Y. Meng, Z.X. Yan, W. Sun, et al., Azoxystrobin disrupts colonic barrier function in mice via metabolic disorders mediated by gut microbiota. J. Agric. Food. Chem. 71 (2023) 789-801. https://doi.org/10.1021/acs.jafc.2c05543.

[46] I.N. Grigor'eva, Gallstone Disease, Obesity and the *firmicutes*/*bacteroidetes* ratio as a possible biomarker of gut dysbiosis. J. Pers. Med. 11 (2021) 13. https://doi.org/10.3390/jpm11010013.

[47] Y.G. Sun, S.S. Zhang, Q.X. Nie, et al., Gut firmicutes: Relationship with dietary fiber and role in host homeostasis. Crit. Rev. Food Sci. Nutr. 63 (2023) 12073-12088. https://doi.org/10.1080/10408398.2022.2098249.

[48] Z.Y. Meng, S. Yan, W. Sun, et al., Chlorothalonil induces obesity in mice by regulating host gut microbiota and bile acids metabolism via FXR pathways. J. Hazard. Mater. 452 (2023) 131310. https://doi.org/10.1016/j.jhazmat.2023.131310.

[49] H.W. Chang, E.M. Lee, Y. Wang, et al., *Prevotella copri* and microbiota members mediate the beneficial effects of a therapeutic food for malnutrition. Nat. Microbiol. 9 (2024) 922–937. https://doi.org/10.1038/s41564-024-01628-7.

[50] C.L. Betancur-Murillo, S.B. Aguilar-Marin, J. Jovel, Prevotella: A key player in ruminal metabolism. Microorganisms 11 (2023) 1. https://doi.org/10.3390/microorganisms11010001.